On Noise Abduction for Answering Counterfactual Queries: A Practical Outlook

Anonymous authors
Paper under double-blind review

Abstract

A crucial step in counterfactual inference is abduction - inference of the exogenous noise variables. Deep Learning approaches model an exogenous noise variable as a latent variable. Our ability to infer a latent variable comes at a computational cost as well as a statistical cost. In this paper, we show that it may not be necessary to abduct all the noise variables in a structural causal model (SCM) to answer a counterfactual query. In a fully specified causal model with no unobserved confounding, we also identify exogenous noises that must be abducted for a counterfactual query. We introduce a graphical condition for noise identification from an action consisting of an arbitrary combination of hard and soft interventions. We report experimental results on both synthetic and real-world German Credit Dataset showcasing the promise and usefulness of the proposed exogenous noise identification.

1 Introduction

"What if?" questions are very frequent to the decision-making system in almost all realms of knowledge. These questions evoke hypothetical conditions usually contradicting the factual evidence. For example, when a patient dies in the hospital, a natural question is: What would have happened if the clinicians acted differently? Another example, had the candidate been male instead of female, would the decision from the admissions committee be more favorable? By and large, counterfactuals are key ingredients that go into explaining why things happened as they did. It is not possible to answer those questions using statistical tools only, but the method of counterfactual inference of hypothetical scenarios can prove helpful in those cases (Pearl, 2016).

Counterfactual techniques have been proposed into deep learning only in recent times (Schölkopf, 2019). For instance, there are inquisition in fairness (Kusner et al., 2017), recourse (Karimi et al., 2021), harm (Richens et al., 2022), mitigating bias in image classifiers (Dash et al., 2022), mitigating language bias in VQA (Niu et al., 2021), Zero-Shot Learning and Open-Set Recognition (Yue et al., 2021), mental health care (Marchezini et al., 2022).

The structural causal model (SCM) is the standard framework for computing the answers to the counterfactual queries. An SCM takes two sets of variables - exogenous and endogenous, and a set of structural assignments into account that assigns each endogenous variable a value according to the values of some other variables in the model. The exogenous variables are external to the model. We chose not to elucidate how they are caused. Each of endogenous variables is a descendant of an exogenous variable. One can use the structural assignments to compute the value of endogenous variables accurately from the values of the exogenous variables. The SCM paradigm provides a three-step procedure for answering counterfactual questions: Abduction, Action and Prediction. Abduction is the tractable inference of the exogenous noise variables. Action is to perform interventions. Prediction is to compute the quantities of interest. Deep Learning approaches founded on these three steps have been introduced for generating counterfactuals very recently. For instance, Pawlowski et al. (2020) employ normalising flows and variational inference for enabling tractable counterfactual inference, Sanchez & Tsaftaris (2022) use diffusion models for counterfactual estimation, Axel Sauer (2021) proposes counterfactual generative networks, Dash et al. (2022) incorporates a structural causal model (SCM) in a variant of Adversarially Learned Inference for generating counterfactual

images. Normalizing flow-based methods for answering counterfactual queries has received a lot of attention in no time. For examples, Pawlowski et al. (2020)'s work on healthy magnetic resonance images of the brain has been extended to account for the clinical and radiological phenotype of multiple sclerosis (MS) by Reinhold et al. (2021). Wang et al. (2021) perform counterfactual inference to achieve harmonization of brain imaging data with different protocols and from different sites in a clinical study.

From a deep learning perspective, an exogenous variable might be considered as an inferred latent variable. To infer the state of the latent noise attached to an endogenous variable, we typically model a normalizing flow, perform amortized variational inference (in the case of very high dimensional variables) (Pawlowski et al., 2020) or use deterministic forward diffusion(Sanchez & Tsaftaris, 2022). Our ability to infer a latent variable comes at a computational cost as well as statistical cost. To illustrate, the framework for counterfactual estimation by inferring exogenous noises via normalising flows parameterizes each structural assignment of an SCM as an invertible mechanism. Each mechanism explicitly calculates its inverse to enable efficient abduction of exogenous noises. These invertible architectures are typically computationally heavy. For a detailed description on normalizing flows, see Papamakarios et al. (2019).

However, given an SCM, in practice we are interested in counterfactual queries involving a few variables (not all)! For an example, Reinhold et al. (2021) studies what would brain image of the subject look like if the subject did not have lesions given the observation that they have a 60 mL lesion load?, while the proposed SCM consists of age, lesion volume of the subject, duration of MS symptoms, slice number, brain volume, biological sex, image, ventricle volume, and the expanded disability severity score. Hence, it is quite natural to ask for noise variables that we can get rid of from abducting. While Pawlowski et al. (2020) have mentioned (on a footnote) in the case of brain imaging example that abduction of the noise attached to 'sex' is not necessary as 'sex' has no causal parents in the SCM[1] (Figure 5, Pawlowski et al. (2020)), we are unaware of any dedicated effort to identify the noises that must be abducted to answer a counterfactual query.

In this context, our work shows that it mayn't be necessary to infer all the noise variables in the SCM and identifies exogenous noise variables that we must infer in order to answer a counterfactual query in a fully specified causal model with no unobserved confounding. We also introduce a graphical condition for noise identification from an action consisting of an arbitrary combination of hard, soft and semi-soft(semi-hard) interventions. We report experimental results on both synthetic and real world German Credit Dataset showcasing the promise and usefulness of the proposed exogenous noise identification. The Code for reproducing the results will be available at Github.

2 Preliminaries

2.1 Background on structural causal models

A structural causal model(SCM) is defined as a tuple $\mathfrak{C} := (\mathcal{S}, \mathbb{P}(\boldsymbol{\epsilon}))$, where $\mathcal{S} = (f_1, f_2, ..., f_p)$ is a collection of p deterministic structural assignments,

$$X_j := f_j(\mathbf{Pa}_j, \boldsymbol{\epsilon}_j), \quad j = 1, 2, .., p, \tag{1}$$

where $\mathbf{Pa}_j \subseteq \{X_1, ..., X_p\} \setminus \{X_j\}$ is the set of parents of X_j (its direct causes) and $\mathbb{P}(\boldsymbol{\epsilon}) = \prod_{i=1}^{p} \mathbb{P}(\boldsymbol{\epsilon}_i)$ is the joint distribution over mutually independent exogenous noise variables. The graph of a structural causal model $\mathfrak{G}$ is obtained simply by drawing directed edges pointing from causes to effects. As assignments are assumed acyclic, the directed graph $\mathfrak{G}$ induced by the SCM $\mathfrak{C}$ is also acyclic. Every SCM $\mathfrak{C}$ entails a unique joint distribution $P^{\mathfrak{C}}_{\mathbf{X}}$ over the variables $\mathbf{X} = (X_1, ..., X_p)$ such that relationships in (1) hold true. The graph structure along with the joint independence of the exogenous noises factorise the entailed distribution $P^{\mathfrak{C}}_{\mathbf{X}}$ canonically into causal conditionals that is referred as causal (or disentangled) factorization,

$$P^{\mathfrak{C}}_{\mathbf{X}}(\mathbf{X} = \mathbf{x}) := \mathbb{P}_{\mathfrak{G}}(\mathbf{x}) = \prod_{j=1}^{p} \mathbb{P}(x_j | \mathbf{pa}^{\mathfrak{G}}_j). \tag{2}$$

[1]This need not be the case always. For instance, example 1(d).

This allows to use $\mathfrak{G}$ for predicting the effects of interventions, defined as substituting one or multiple of its structural assignments, written as '$do(\cdots)$'.

An intervention on a set of variables $\{X_t : t \in I\}$ is defined as substituting the respective structural assignments by

$$X_t := \tilde{f}_t(\widetilde{\mathbf{Pa}}_t, \tilde{\boldsymbol{\epsilon}}_t), \quad t \in I.$$

The entailed distribution in the new SCM $\tilde{\mathfrak{C}}$ is called as intervention distribution, denoted by $P^{\tilde{\mathfrak{C}}}_{\mathbf{X}}$. The set of exogenous variables $\{\boldsymbol{\epsilon}_t : t \notin I\} \cup \{\tilde{\boldsymbol{\epsilon}}_t : t \in I\}$ in $\tilde{\mathfrak{C}}$ are required to be mutually independent. An intervention, where the structural assignment for a variable is modified by changing the function or the noise term, resulting a change in the conditional distribution given its parents, is called soft/imperfect intervention. It is written as $do(X_t := \tilde{f}_t(\widetilde{\mathbf{Pa}}_t, \tilde{\boldsymbol{\epsilon}}_t))$ (Peters et al., 2017). As the new SCM $\tilde{\mathfrak{C}}$ should have an acyclic graph, the set of allowed interventions thus depends on the graph $\mathfrak{G}$, induced by $\mathfrak{C}$. In this paper, we mainly focus on interventions with $\widetilde{\mathbf{Pa}}_t$ equals $\mathbf{Pa}_t$ or empty (that will be clear from the context) and we use $\widetilde{\mathbf{Pa}}_t$ for a very different purpose described in section 3. Independent Causal Mechanisms (ICM) Principle (Peters et al. (2017)) tells that performing an intervention upon one mechanism $\mathbb{P}(X_i|\mathbf{Pa}_i)$ does not change any of the other mechanisms $\mathbb{P}(X_j|\mathbf{Pa}_j)(i \neq j)$. As a consequences, we get

$$P^{\tilde{\mathfrak{C}}}_{\mathbf{X}}(\mathbf{X} = \mathbf{x}) := \mathbb{P}_{\tilde{\mathfrak{G}}}(\mathbf{x}) = \prod_{j \notin I} \mathbb{P}_{\mathfrak{G}}(x_j|\mathbf{pa}^{\mathfrak{G}}_j) \prod_{j \in I} \mathbb{P}_{\tilde{\mathfrak{G}}}(x_j|\widetilde{\mathbf{pa}}^{\tilde{\mathfrak{G}}}_j). \tag{3}$$

When $\tilde{f}(\widetilde{\mathbf{Pa}}_t, \tilde{\boldsymbol{\epsilon}}_t)$ puts a point mass on a real value a, i.e., $\mathbb{P}_{\tilde{\mathfrak{G}}}(x_t|\widetilde{\mathbf{pa}}_t) = \mathbf{1}_{x_t=a}$, we simply written it as $do(X_t = a)$ and call this an atomic/hard/perfect intervention. In particular, such constant reassignment disconnects X_t from all its parents and imparts a direct manipulation disregarding its natural causes.

2.2 Counterfactuals

Given an observed outcome, counterfactuals are hypothetical retrospective interventions (cf. potential outcome): 'Given that we observed $(X_i, X_j) = (x^{obs}_i, x^{obs}_j)$, what would X_i have been if X_j were x'_j? By assumption, the state of any observable variable is fully determined by the exogenous noises and structural assignments/equations. The unit-level counterfactual is defined as the solution for X_i for a given situation $\boldsymbol{\epsilon} = \epsilon$ where the equations for X_j is replaced with $X_j = x'_j$. We denote it by $X_{i X_j \leftarrow x'_j}(\epsilon)$ (Read: "The value of X_i in situation ϵ, had X_j been x_j"). We might be able to answer unit-level (or individual-level) counterfactual queries if we know specific functional form of these structural equations. Mathematically, counterfactual inference can be formulated as : (Pearl (2009))

1. **Abduction:** Predict the exogenous noise $\boldsymbol{\epsilon}$ from the observations $\mathbf{x}^{obs}$, i.e., infer $\mathbb{P}(\boldsymbol{\epsilon}|\mathbf{X} = \mathbf{x}^{obs})$.
2. **Action:** Perform interventions (e.g. $do(X_j = x'_j)$) corresponding to the desired manipulations, resulting in a modified SCM $\tilde{\mathfrak{C}} := \mathfrak{C}|_{\mathbf{X}=\mathbf{x}^{obs}; do(X_j=x'_j)} = (\tilde{S}, \mathbb{P}(\boldsymbol{\epsilon}|\mathbf{X} = \mathbf{x}^{obs}))$, where $\tilde{S}$ is the collection of structural assignments modified by interventions.
3. **Prediction:** Compute the quantities of interest (e.g. $X_{i X_j \leftarrow x'_j}(\epsilon)$) based on the distribution entailed by the counterfactual SCM $\tilde{\mathfrak{C}}$, denoted by $P^{\tilde{\mathfrak{C}}}_{\mathbf{X}} = P^{\mathfrak{C}|_{\mathbf{X}=\mathbf{x}^{obs}; do(X_j=x'_j)}}_{\mathbf{X}}$.

The updated noise distribution of exogenous variables $\mathbb{P}(\boldsymbol{\epsilon}|\mathbf{X} = \mathbf{x}^{obs})$ need not be mutually independent anymore. It is not always possible determine the counterfactuals with probability 1. When we can't solve for $\boldsymbol{\epsilon}_i$ (e.g. function f_i that maps $\boldsymbol{\epsilon}_i$ to X_i for a fixed value of $\mathbf{x}$ isn't invertible in noise term?), we assume some prior distribution for $\boldsymbol{\epsilon}_i$ and update $\mathbb{P}(\boldsymbol{\epsilon}_i)$ by observations $\mathbf{x}^{obs}$ to obtain $\mathbb{P}(\boldsymbol{\epsilon}_i|\mathbf{x}^{obs})$ (**Abduction**). In general, using Bayes' theorem,

$$\mathbb{P}(\boldsymbol{\epsilon} = \epsilon|\mathbf{X}(\boldsymbol{\epsilon}) = \mathbf{x}^{obs}) = \frac{\mathbf{1}_{\mathbf{X}(\epsilon)=\mathbf{x}^{obs}} \mathbb{P}(\boldsymbol{\epsilon} = \epsilon)}{\sum_{\{\epsilon'|\mathbf{X}(\epsilon')=\mathbf{x}^{obs}\}} \mathbb{P}(\boldsymbol{\epsilon} = \epsilon')}. \tag{4}$$

$\mathbf{X}(\boldsymbol{\epsilon})$ emphasizes the fact that every endogenous variable X_i is a function of $\boldsymbol{\epsilon}$. In the case of non-invertible structural assignments, we don't get all the probabilities concentrated on one particular value of counterfactual $X_{iX_j \leftarrow x'_j}(\epsilon)$, rather we get a distribution. Averaging over the space of $\boldsymbol{\epsilon}$, a potential outcome $X_{iX_j \leftarrow x'_j}(\epsilon)$ induces a random variable that is simply denoted as $X_{iX_j \leftarrow x'_j}$. The counterfactual distribution $\mathbb{P}(X_{iX_j \leftarrow x'_j} = X_{iX_j \leftarrow x'_j}(\epsilon) | X_j = x_j^{obs}, X_i = x_i^{obs})$ denotes the probability that $X_{iX_j \leftarrow x'_j}$ is equal to the value $X_{iX_j \leftarrow x'_j}(\epsilon)$ if X_j is changed to a different value x'_j, given a specific observation $X_i = x_i^{obs}$ and $X_j = x_j^{obs}$. Let $\boldsymbol{\epsilon} = \epsilon$ be one of the situation that leads to the observation $\mathbf{X} = \mathbf{x}^{obs}$ (more specifically, $X_i = x_i^{obs}, X_j = x_j^{obs}$). Then, in particular,

$$\mathbb{P}(X_{iX_j \leftarrow x'_j} = X_{iX_j \leftarrow x'_j}(\epsilon) | X_j = x_j^{obs}, X_i = x_i^{obs}) = \mathbb{P}(\boldsymbol{\epsilon} = \epsilon | \mathbf{X} = \mathbf{x}^{obs}).$$

It advances us from unit-level counterfactual to population-level counterfactual that is not specific to a situation ϵ, e.g., $\mathbb{E}(X_{iX_j \leftarrow x'_j} | X_j = x_j)$. Expectation is taken over the whole population. $\mathbb{P}(\boldsymbol{\epsilon})$ defines a probability distribution over endogenous variables $\mathbf{X}$,

$$\mathbb{P}(X_i = x_i) = \sum_{\{\epsilon | X_i(\epsilon) = x_i\}} \mathbb{P}(\boldsymbol{\epsilon} = \epsilon).$$

The probability of counterfactual statements is defined in the same manner, e.g.,

$$\begin{aligned} \mathbb{P}(X_{iX_j \leftarrow x'_j} = x'_i | X_j = x_j^{obs}, X_i = x_i^{obs}) &= \sum_{\{\epsilon | X_{iX_j \leftarrow x'_j}(\epsilon) = x'_i\}} \mathbb{P}(\boldsymbol{\epsilon} = \epsilon | \mathbf{X} = \mathbf{x}^{obs}) \\ &= \sum_{\epsilon} \mathbb{P}(X_{iX_j \leftarrow x'_j}(\epsilon) = x'_i) \mathbb{P}(\boldsymbol{\epsilon} = \epsilon | \mathbf{X} = \mathbf{x}^{obs}) \end{aligned} \tag{5}$$

With the help of such formulation, we are allowed to compute joint probabilities of every combination of counterfactual and observable events. Natural direct and indirect effects in mediation analysis, probability of necessity, probability of sufficiency (Pearl, 2016), harm (Richens et al., 2022), etc. are few examples of counterfactuals quantities.

2.2.1 Identifiability of counterfactuals

One fundamental question in counterfactual analysis is the question of identification: Can the counterfactual quantities be estimated from either observational or experimental data or both the observational data and the experimental data? In general, it is not immediately clear how to design effective experimental procedures for evaluating counterfactuals, or how to compute them from observational data. In a causal model with joint distribution having joint density satisfying 2, if all parameters of the causal model are known (including $\mathbb{P}(\boldsymbol{\epsilon})$), each and every counterfactual is identifiable and can be computed using the three steps - abduction, action, and prediction. Standard tools of the SCM framework don't inherently restrict intervention. one could at least in theory intervene unconditionally on any subset of variables to perform counterfactual analysis. Thus the choice of form and feasibility in the scope of intervention are delegated to the individual and\or the institution and made based on a semantic understanding of the modelled variables. For an example, Z can't be intervened in causal graphs in Figure 2 in Zhang et al. (2020). Throughout this paper we don't restrict ourselves from intervening on the variables of interest in the counterfactual query.

For computing unit-level counterfactuals one needs parametric forms of structural assignments. Flow-based SCMs use normalizing flows to parameterize each structural assignment of an SCM as an invertible mechanism. To answer population-level counterfactuals, one doesn't require parametric forms of structural equations. See Malinsky et al. (2019) for general identification of counterfactual quantities.

3 Counterfactual with different interventions

In section 2.1, we mentioned soft interventions, where the original conditional distributions of the intervened variables are replaced with new ones, without fully eliminating the causal effect of the parents. This operation is also known as a mechanism change (Tian & Pearl (2013)). It presents in many settings a more

realistic model than hard or perfect interventions, where variables are forced to a fixed value. Karimi et al. (2021) and Crupi et al. (2021) perform soft interventions (particularly, an additive intervention) to generate counterfactual explanation and recommendation in the context of algorithim recourse.

Example 1 (adapted from Example 6.18 in Peters et al. (2017))**.** *Consider the following SCM:*

$$X := \epsilon_X + 1$$
$$Y := X^2 + \epsilon_Y$$
$$Z := 2Y + X + \epsilon_Z$$

with $\epsilon_X, \epsilon_Y, \epsilon_Z \sim$ *Uniform*$(\{-5, -4, ..., 4, 5\})$ *idenpendently. Now, assume that we observe* $(X, Y, Z) = (1, 2, 4)$ *and we are interested in the counterfactual query(a): what would have been* Z*, had* Y *been 5? Now we pose the question as following:*

To answer the counterfactual query, do we need to know the state of the ϵ_X*?*

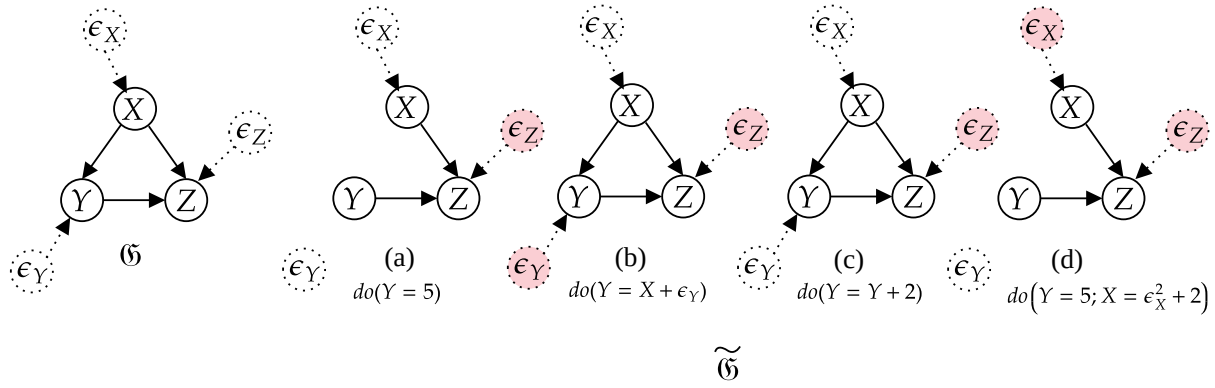

Figure 1: Left-most directed acyclic graph (dag) $\mathfrak{G}$ is the causal graph induced by the SCM in example 1. The rest four are causal graph induced by counterfactual SCMs for queries in (a),(b),(c) & (d). Noises that must be abducted are filled in pink

Note that, given observation $(X, Y, Z) = (1, 2, 4)$*, inferring* $\epsilon_Z = -1$ *is sufficient to answer* $Z_{Y \leftarrow 5}(\epsilon) = 10$*. Furthermore, We don't even need to know the structural equations of* X *and* Y*. However, the scenario would be a bit different if we change the counterfactual question(b): What would have been* Z*, had* Y *followed* $Y := X + \epsilon_Y$ *? In this case, given observation* $(X, Y, Z) = (1, 2, 4)$*, we need to infer* $\epsilon_Z = -1$ *and* $\epsilon_Y = 1$ *to answer that* Z *would have been* 4*, had* Y *followed the structural equation* $Y := X + \epsilon_Y$*. Further, for computing* $Z_{Y \leftarrow Y+2}(\epsilon) = 8$ *(c), we don't even need to infer* ϵ_Y*. Only* ϵ_Z *suffices. Here, an interesting observation to make is that the dag* $\tilde{\mathfrak{G}}$ *of the manipulated SCM* $\tilde{\mathfrak{C}}$ *remains same as* $\mathfrak{G}$ *for the counterfactual quarries in (b) and (c) (figure 1). To illustrate more, consider the counterfactual question (d): What would have been* Z*, had* Y *been 5 and* X *followed* $X := \epsilon_X^2 + 2$ *? To answer this, it is sufficient to infer* $(\epsilon_X, \epsilon_Z) = (0, -1)$*. Had* Y *been 5 and* X *followed* $X := \epsilon_X^2 + 2$*,* Z *would have been 11.*

The above example motivates us to define semi-hard\semi-soft intervention, an intermediate scenario where we technically don't force a constant value but disregard the interventions on the ancestor variables (of the intervened variable) when we intervene. Intervention is defined to take a special functional form and as a result, it is not required to know intervened variable's parents and corresponding noise variable for computing the value of the intervention if we are given observed value.

Definition 1 (semi-soft\semi-hard intervention)**.** *An intervention on* X_t *of the form* $X_t \leftarrow \tilde{f}(\mathbf{Pa}_t, \boldsymbol{\epsilon}_t) = h(f(\mathbf{Pa}_t, \boldsymbol{\epsilon}_t))$*, where* h *is any arbitrary function, is called semi-soft\semi-hard intervention.*

$\mathbf{Pa}_t$ emphasizes the fact that we disregard any intervention on ancestors of X_t. If we consider the intervention on ancestors, we would have written it with $\widetilde{\mathbf{Pa}_t}$ and that coincides with soft-intervention. A concrete

example is given in appendix A.1. An typical additive interventions is an example of semi-soft intervention ($h(f) = f + c$, where c is a constant). Hard interventions are also a special case of semi-soft interventions ($h(f) = c$) but in this article, we strictly differentiate between a hard intervention, a soft intervention and a semi-soft intervention. One may argue that since we are denying interventional changes on ancestors when we are intervening, we could disconnect a semi-hard intervened variable from its parents in the graph induced by interventions. In-fact, for the sake of keeping things simple, we take resort of this for rest of the paper.

4 Notations and problem setup

A path in $\mathfrak{G}$ is a sequence of (at least two) distinct vertices $X_{i_k}, ..., X_{i_m}$, such that there is an edge between X_{i_k} and X_{i_m} for all $k = 1, ..., (m-1)$. If $X_{i_k} \to X_{i_{k+1}}$ for all k, we speak of a directed path from X_{i_1} to X_{i_m}. We will use the following standard kinship relations for sets of vertices in a directed acyclic graph $\mathfrak{G}$:

$\mathbf{De}_i^{\mathfrak{G}} = \{X_j : \exists$ a directed path from X_i to X_j in $\mathfrak{G}\}$
$\mathbf{De}_A^{\mathfrak{G}} = \{X_j : \exists$ a directed path to X_j from X_i in $\mathfrak{G}$, for any $i \in A\}$
$\mathbf{An}_i^{\mathfrak{G}} = \{X_j : \exists$ a directed path from X_j to X_i in $\mathfrak{G}\}$
$\mathbf{An}_A^{\mathfrak{G}} = \{X_j : \exists$ a directed path from X_j to X_i in $\mathfrak{G}$, for any $i \in A\}$

Given an index set $\mathcal{C} \subseteq \{1, 2, ...p\}$, $\mathbf{X}_{\mathcal{C}}$ denotes the random vector $(X_i)_{i \in \mathcal{C}}$ and $\mathbf{X}_{-\mathcal{C}} = (X_i)_{i \notin \mathcal{C}}$. Let us formally state the problem we want to address. Assume $\mathfrak{C} := (\mathcal{S}, \mathbb{P}(\boldsymbol{\epsilon}))$ be a structural causal model. The graph of $\mathfrak{C}$ is $\mathfrak{G}$. For ensuring identifiability , we assume that $\mathfrak{C}$ satisfies four standard assumptions: the markov property, causally sufficiency (i.e., no hidden confounders) causal minimality and causal faithfulness (Peters et al. (2017)). Assume A_H be the index set of random variables on which we perform hard interventions in action stage. Similarly, $\{X_i : i \in A_S\}$ and $\{X_i : i \in A_T\}$ be the set of random variables on which we act soft interventions and semi-hard\semi-soft interventions, respectively. $A = A_S \cup A_H \cup A_T$ be the index set of intervened variables. Let the counterfactual query we want to answer be $\mathcal{Q}$:

What would $\mathbf{X}_{\mathcal{C}}$ have been if $\mathbf{X}_{A_H}$ were $\mathbf{x}_{A_H}$ and for each $i \in A_S \cup A_T$, mechanism f_i was changed to $\tilde{f}_i$, given that we observe $\mathbf{X} = \mathbf{x}^{obs}$?

For the sake of simplicity, we denote the intervention

$$do\Big(X_j = x_j \text{ for } j \in A_H; X_j = \tilde{f}_j(\mathbf{Pa}_j, \boldsymbol{\epsilon}_j) \text{ for } j \in A_S \cup A_T\Big)$$

as $do(\mathcal{A} \leftarrow \mathfrak{a})$. $\tilde{\mathfrak{G}}$ be the graph of counterfactual SCM $\tilde{\mathfrak{C}}$, modified by intervention $do(\mathcal{A} \leftarrow \mathfrak{a})$. For $i \in \mathcal{C}$, let $X_{i\,\mathcal{A} \leftarrow \mathfrak{a}}$ denotes an answer to the counterfactual query $\mathcal{Q}$.

5 Noises that are important to $\mathcal{Q}$

Observation 1. *If we intervene on X_j, following the causal flow in the DAG $\mathfrak{G}$, only X_j and the descendants of X_j, $\mathbf{De}_j^{\mathfrak{G}}$ will get affected*[2]*.*

Theorem 1. *$X_{i\,\mathcal{A} \leftarrow \mathfrak{a}} = x_i^{obs}$ almost surely, for $i \in \mathcal{C} \setminus \{k : X_k \in \mathbf{De}_A^{\mathfrak{G}} \cup \mathbf{X}_A\}$.*

Proof. Consider the subgraph $\mathcal{G}$ of $\mathfrak{G}$, obtained by deleting the vertices in $\{X_k : X_k \in \mathbf{De}_A^{\mathfrak{G}}\} \cup X_A$. $\tilde{\mathfrak{G}}$ be the graph induced by the SCM $\tilde{\mathfrak{C}}$, modified by the intervention $do(\mathcal{A} \leftarrow \mathfrak{a})$. By observation 1, for any $i \in \{k : X_k \in \mathcal{G}\}$, the triplet $(f_i, \mathbf{Pa}_i^{\mathcal{G}}, \mathbf{An}_i^{\mathcal{G}})_{\mathfrak{C}}$ is same as $(f_i, \mathbf{Pa}_i^{\tilde{\mathfrak{G}}}, \mathbf{An}_i^{\tilde{\mathfrak{G}}})_{\tilde{\mathfrak{C}}}$, where $(f_i, \mathbf{Pa}_i^{\mathcal{G}}, \mathbf{An}_i^{\mathcal{G}})_{\mathfrak{C}}$ denotes the triplet of the structural assignment f_i in the SCM $\mathfrak{C}$, parents and ancestors of X_i in a subgraph $\mathcal{G}$ of $\mathfrak{G}$, respectively. Let $\boldsymbol{\epsilon} = \epsilon$ be one of the situations that leads to the observation $\mathbf{X} = \mathbf{x}^{obs}$, in particular $X_i = x_i^{obs}$. Then, following a topological order in $\mathfrak{G}$,

$$X_i(\epsilon) = x_i^{obs} = f_i(\mathbf{pa}_i, \epsilon_i) = X_{i\,\mathcal{A} \leftarrow \mathfrak{a}}(\epsilon), \quad \forall i \in \{k : X_k \in \mathcal{G}\}.$$

[2]By 'get affected', we mean a distributional change.

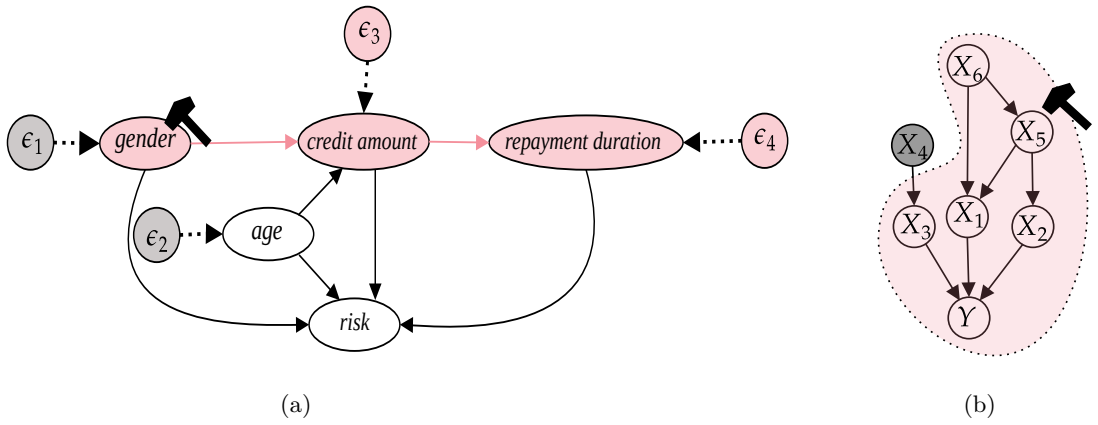

(a) (b)

Figure 2: (a) Causal graph for the German credit dataset. (b) Causal graph of the synthetic dataset.

Hence,

$$\{\epsilon : X_i(\epsilon) = x_i^{obs}\} = \{\epsilon' : X_{i_{A\leftarrow a}}(\epsilon') = x_i^{obs}\}, \quad \forall i \in \{k : X_k \in \mathcal{G}\}.$$

Using (4) and (5), we get

$$\mathbb{P}(X_{i_{\mathcal{A}\leftarrow \mathfrak{a}}} = x_i^{obs} | \mathbf{X} = \mathbf{x}^{obs}) = 1, \quad \forall i \in \{k : X_k \in \mathcal{G}\}.$$

We get the desired result as $\mathcal{C} \setminus \{k : X_k \in \mathbf{De}_A^{\mathfrak{G}} \cup \mathbf{X}_A\} \subseteq \{k : X_k \in \mathcal{G}\}$.

□

As an immediate consequence, we don't need to infer noises attached to the variables outside the action set $\mathbf{X}_A$ and its descendants $\mathbf{De}_A^{\mathfrak{G}}$, as we are about to modify the SCM $\mathfrak{C}$ by acting on variables in A. For example, in the causal graph of figure 2a, if we intervene (hypothetically, in theory) on 'gender', a counterfactual answer about 'age' won't be a diversion from what we observe, which is pretty much intuitive from the causal graph and indeed 'causal' in nature. On the other hand, we are interested in counterfactual queries about $\mathbf{X}_\mathcal{C}$. We do not need to oversee all the variables in $\mathbf{De}_A^{\mathfrak{G}} \cup \mathbf{X}_A$.

Theorem 2. *Let X_j hasn't been intervened. Then X_j is affected in 'counterfactual' iff atleast an ancestor of X_j has been intervened.*

Proof. If we intervene on an ancestor of X_j, from observation 1, X_j is affected in 'counterfactual'. For the only if part, assume none of the ancestor of X_j has been intervened. Let I be the index set of intervened variables then $X_j \notin \mathbf{De}_I^{\mathfrak{G}}$. Moreover, as X_j hasn't been intervened on, by theorem 1 the counterfactual value of X_j remains same as its observed value, contradicting the hypothesis.

□

Theorem 2 tells us that we need to worry about noises attached to variables in $\mathbf{An}_\mathcal{C}^{\mathfrak{G}}$ only, as we are interested in a counterfactual query about $\mathbf{X}_\mathcal{C}$. For example, if we are concerned about only 'repayment duration' in the causal graph of figure 2a, we need to take care of its ancestors' exogenous noise. Furthermore, theorem 1 and theorem 2 allow us to constrain the search space to all the exogenous noises correspond to the variables lying on a directed path from $\mathbf{X}_A$ to $\mathbf{X}_\mathcal{C}$ in $\mathfrak{G}$. Continuing with the example of figure 2a, if we are interested in 'repayment duration' and we are intervening on 'gender' in the action step, we only need to infer ϵ_3 and ϵ_4 as they are attached to the variables that lie on the directed path (coloured in pink) from 'gender' to 'repayment duration'. Then why do we exclude ϵ_1 from abduction?

Theorem 3. $X_{j_{X_j\leftarrow x'_j}} = x'_j$.

Proof. Immediate from property 2 (Effectiveness) Pearl (2009). □

Effectiveness property releases us from inferring $\boldsymbol{\epsilon}_{A_H}$. By definition of semi-soft intervention, we don't need to infer $\boldsymbol{\epsilon}_{A_T}$. As the hard interventions and the semi-soft\semi-hard disconnect parents from the intervened variables, we further filter out exogenous disturbances by looking at $\tilde{\mathfrak{G}}$, instead of $\mathfrak{G}$.

Theorem 4. $\mathbf{X}_{\mathcal{C}\,\mathcal{A}\leftarrow\mathfrak{a}}(\boldsymbol{\epsilon}) = \mathbf{X}_{\mathcal{C}\,\mathcal{A}\leftarrow\mathfrak{a};do^*_{\mathcal{A}}}(\boldsymbol{\epsilon})$, *where* $do^*_{\mathcal{A}} = do\Big(X_i = x_i^{obs}$ *for* $X_i \in \mathbf{An}^{\tilde{\mathfrak{G}}}_{\mathcal{C}} \setminus \{\mathbf{De}^{\tilde{\mathfrak{G}}}_{A} \cup \mathbf{X}_A\}\Big)$.

Proof. Immediate from theorem 1 and property 1 (Composition) Pearl (2009) . □

Theorem 4 allows us to intervene on the variables outside $\mathbf{De}^{\tilde{\mathfrak{G}}}_{A} \cup \mathbf{X}_A$ with their observed values. This intervention $do^*_{\mathcal{A}}$ depends on the intervention $do(\mathcal{A} = \mathfrak{a})$. Theorem 4 also guarantees that $do^*_{\mathcal{A}}$ doesn't change unit-level counterfactuals. We discuss this idea of intervention with the observation in appendix A.2 in more details. We devise the following four-step procedure (adding one more to Pearl (2009)) for computing a counterfactual query $\mathcal{Q}$ in the SCM framework:

1. **Pre-abduction:** Identify the acting interventions, $do(\mathcal{A} \leftarrow \mathfrak{a})$. Identify the ϵ_i's that are essential to answer $\mathcal{Q}$, by looking at all the directed path from $\mathbf{X}_A$ to $\mathbf{X}_{\mathcal{C}}$ in the graph $\tilde{\mathfrak{G}}$, modified by the $do(\mathcal{A} \leftarrow \mathfrak{a})$ and the type of the interventions on $\mathbf{X}_A$.
2. **Abduction:** Predict the essential exogenous noises, ϵ_i's from the observations $\mathbf{x}^{obs}$, i.e., infer $\mathbb{P}(\pi_{\mathcal{A}}(\boldsymbol{\epsilon})|\mathbf{X} = \mathbf{x}^{obs})$, where $\pi_{\mathcal{A}}$ is a projection operator depends on $do(\mathcal{A} \leftarrow \mathfrak{a})$.
3. **Action:** Perform the desired interventions $do(\mathcal{A} \leftarrow \mathfrak{a}), do^*_{\mathcal{A}}$.
4. **Prediction:** Compute the quantities of interest in $\mathcal{Q}$.

What pre-abduction says is that - we know the interventions we are going to perform. Hence a priori we know causal graph modified by the interventions. So it suggests to exploit this a priori knowledge for noise abduction since ultimately we perform prediction step following these interventions and modified causal graph. This exploitation reduces the number of noises needed to abduct from the number of nodes in $\mathfrak{G}$ to the total number of nodes in all directed paths from $\mathbf{X}_A$ to $\mathbf{X}_{\mathcal{C}}$ in $\tilde{\mathfrak{G}}$. This is quite effective in causal graphs $\mathfrak{G}$ consists of moderate or large number of nodes (variables).

6 Experiments

6.1 Case study 1: synthetic dataset

For the synthetic setting, we generate data following the model in figure 2b, where we assume

$$
\begin{aligned}
&X_6 = \epsilon_6 - 1, && X_5 = 3X_6 + \epsilon_5 - 1, && X_4 = 2\epsilon_4 + 1,\\
&X_3 = -3X_4 + \epsilon_3 - 3, && X_2 = X_5 - \epsilon_2, && X_1 = X_6 - X_5 + 3\epsilon_1,\\
& && Y = X_1 + 2X_2 - 3X_3 + \epsilon_Y, &&
\end{aligned}
$$

and $\epsilon_Y, \epsilon_i \sim \mathcal{N}(0,1)$ independently, for $i = 1, 2..., 6..$ We generate 20000 data points from the SCM. This simple dataset allows for a comparison of generated counterfactuals in a controlled and measurable environment. We consider two models to answer: "What would have happened to Y, if X_5 was different than what we observed: $\mathbf{X} = \mathbf{x}^{obs}, Y = y^{obs}$. Full model infers all the exogenous noises whereas partial model only infers ϵ_1, ϵ_2 and ϵ_Y (following pre-abduction). We use this setting to study the importance of noise identification for abduction.

We use affine coupling flows (Dinh et al., 2017) for X_4 and X_6 and conditional affine coupling transform for other dependent variables. In full model, seven flows are implemented - two linear flows and five conditional

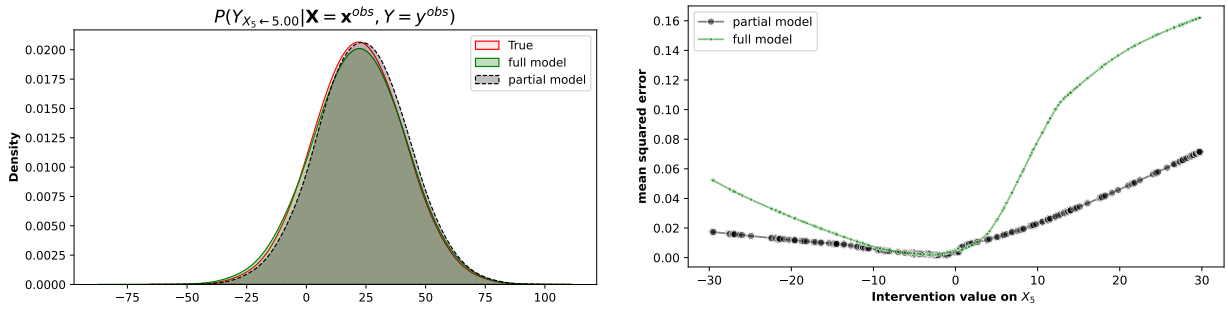

(a) (b)

Figure 3: (a) The red curve is the kernel density estimate (KDE) plot of the true counterfactual distribution. The green solid line and the black dashed lines are the KDE plots of the distributions estimated by the full model and the partial model respectively. (b) Mean squared errors in estimating counterfactual values of Y. The x-axis represents the values we intervene on X_5 Black circles are errors in the partial model. Green dots are errors in the full model.

flows. Whereas in the partial model, only three conditional flows are used for X_1, X_2 and Y respectively. We model base densities with standard gaussian.

We use the Pyro[Bingham et al. (2019)] probabilistic programming language (PPL) framework for implementation of the flow based SCM. A PPL is a programming language in which probabilistic models are specified and inference for these models is performed automatically with terms corresponding to sampling and conditioning. Pyro is a PPL based on PyTorch [Paszke et al. (2019)]. For a detailed overview of PPLs, see van de Meent et al. (2018). Adam (Kingma & Ba, 2015) with batch-size 128, initial learning rate of 10^{-3} is used for optimization purpose. Both models are trained for 1000 epochs using 12th Gen Intel(R) Core(TM) i9-12900KF cpu.

Figure 3a shows the counterfactual distributions $\mathbb{P}(Y_{X_5 \leftarrow 5} | \mathbf{X} = \mathbf{x}^{obs}, Y = y^{obs})$ estimated by full model and the partial model along with the true counterfactual distribution. We intervene X_5 with 200 different values uniformly sampled from -30 to 30. Mean squared errors in counterfactual estimation (on seen datapoints[3]) for each models for the 200 different intervention values has been depicted in figure 3b. We see a significant difference in the training time. Full model takes 11.41 min while partial model takes 6.50 min to train 1000 epochs.

We quantitatively compare the associative capabilities of both models by log-likelihoods (validation) as shown in the table 1. Figures depicting goodness of noise estimation and sampling capabilities of both models are provided in the appendix B.

Table 1: Best validation log-likelihood for full and partial model.

Model	**Log-likelihood**						
	X_6	X_5	X_4	X_3	X_2	X_1	Y
Partial	—	—	—	—	**-1.4160**	**-2.5050**	**-1.4415**
Full	-1.4198	-1.4166	-2.1126	-1.4229	-1.4163	-2.5050	-1.4418

6.2 Case study 2: german credit dataset

As a real-world setting, we consider a subset of the features in the german credit dataset. This subset includes gender (X_1), age (X_2), credit amount (X_3) and repayment duration (X_4). In figure 2a, we see an

[3]By 'seen datapoints', we mean these are the datapoints used in training and validation. MSE in estimation of counterfactuals on unseen data points(test MSE) is given in appendix B

example of DAG representing the causal relationships (Karimi et al. (2021)) in the german credit dataset (Dua & Graff (2017)). We don't consider the risk variable in our experiment. We are interested in studying the counterfactual query: Had the person been male instead of female (or female instead of male), would the person has been offered more (or less) credit amount for a larger (or shorter) duration?

First, flow-based SCM is trained using the observed data. Next, the state of exogenous noises are inferred with the estimated structural assignments that are invertible (abduction step). Then we intervene upon the sex by replacing sex variable with a specific value 'male' or 'female', this is denoted by do(sex = male) or do(sex=female). We use the modified flow-based SCM to compute counterfactual quantities. Similar to synthetic data experiment, we consider two models. Full model infers all the exogenous noise variables except ϵ_1, since we model the mechanisms of gender\sex(X_1) as,

$$x_1 = f_1(\epsilon_1) = \epsilon_1.$$

Age X_2, Credit amount X_3 and repayment duration X_4 are modelled as

$$\begin{aligned}
x_2 &= f_2(\epsilon_2) = (\text{Spline}_\theta \circ \text{AffineNormalisation} \circ \exp)(\epsilon_2), \\
x_3 &= f_3(\epsilon_3; x_1, x_2) = (\text{ConditionalTransform}_\theta([x_1, x_2]) \circ \text{AffineNormalisation} \circ \exp)(\epsilon_3), \\
x_4 &= f_4(\epsilon_4; x_3) = (\text{ConditionalTransform}_\theta([x_3]) \circ \text{AffineNormalisation} \circ \exp)(\epsilon_4).
\end{aligned}$$

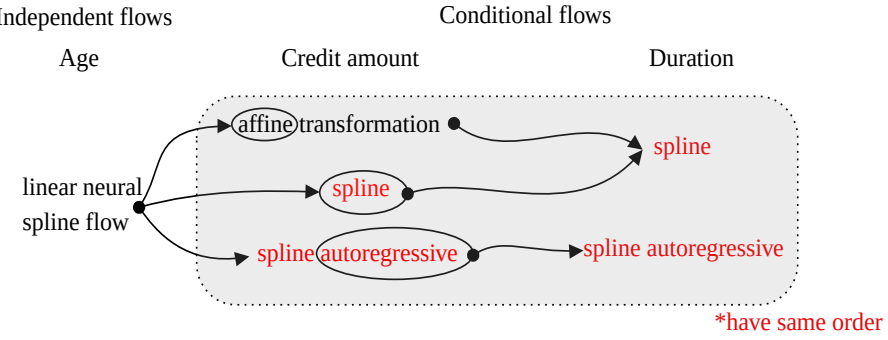

Figure 4: Combinations of flows used in the experiment. Flows' combinations are identified by the phrases inside the ellipse. Flows inside the light grey rectangle are used in the partial model, i.e., we don't model any flow for age in the case of the partial model. We have the same order (i.e., either linear or quadratic) for the flows in red.

The modules highlighted by θ are parameterized using neural networks. We use a categorical distribution for sex (X_1) and directly learn the binary probability of sex (X_1). The density of exogenous noises (except ϵ_1) are standard gaussians. For other structural assignments, we use real-valued normalizing flows. A linear flow and two conditional flows (conditioned on activations of a fully-connected network, one takes age and sex as input for credit amount and another takes credit amount as input for duration) are used as structural assignments for age ,credit amount and duration features respectively. We constrain age (X_1), credit amount (X_3) and repaymaent duration (X_4) variables with lower bound (exponential transform) and rescale it using fixed affine transform for normalization.

Partial model infers only ϵ_3 and ϵ_4 as suggested by pre-abduction (described in section 5). We model flows for credit amount (X_4) and repayment duration (X_3) similar to the full model. But we don't model a flow for the age variable. Combinations of flows used in the experiment are depicted in the figure 4.

Spline_θ transformation stands for the linear neural spline flows (Dolatabadi et al. (2020).) $\text{ConditionalTransform}_\theta(\cdot)$ can be conditional affine or conditional spline transform. We use linear (Dolatabadi et al. (2020)) and quadratic (Durkan et al. (2019)) order, autoregressive and linear neural spline flows for the conditional spline transform. These are more expressive in comparison to the affine flows. Taking $\cdot$ as

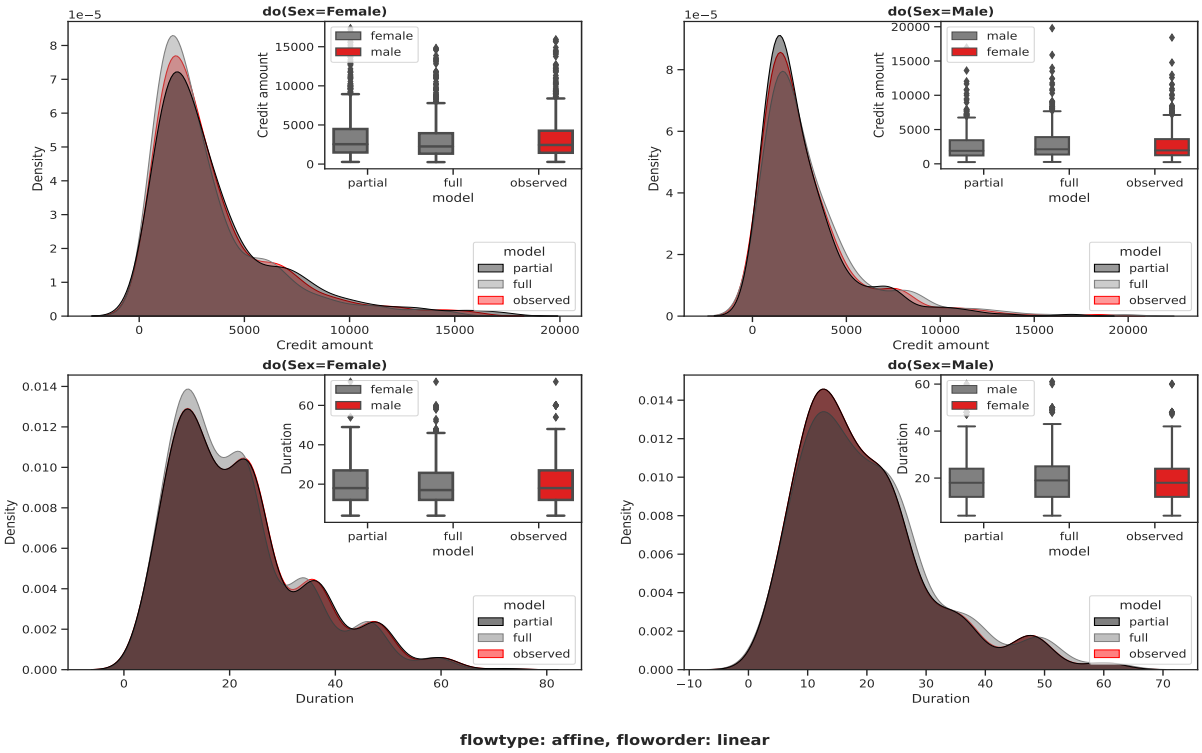

Figure 5: On the left, KDE plots of the observed distributions $P(\text{Credit amount}|\text{Sex} = \text{male})$ and $P(\text{Repayment duration}|\text{Sex} = \text{male})$ are given in red. Counterfactual distributions $P(\text{Credit amount}_{do(\text{Sex=female})}|\text{Sex} = \text{male})$, $P(\text{Repayment duration}_{do(\text{Sex=female})}|\text{Sex} = \text{male})$ estimated by full and partial models are presented in gray and black, respectively. On the right, KDE plots of the observed distributions $P(\text{Credit amount}|\text{Sex} = \text{female})$ and $P(\text{Repayment duration}|\text{Sex} = \text{female})$ are given in red. Counterfactual distributions, $P(\text{Credit amount}_{do(\text{Sex=male})}|\text{Sex} = \text{female})$ and $P(\text{Repayment duration}_{do(\text{Sex=male})}|\text{Sex} = \text{female})$, estimated by full and partial models, are presented in gray and black, respectively. Upper panel is for distributions related to credit amounts. Lower panel is for distributions related to payment duration. Box plots at the right-hand corner of each subplot are self-explanatory.

input, a context neural network estimates the transformation parameters of the ConditionalTransform$_\theta(\cdot)$. We implement the context networks as fully-connected networks for spline and affine flows.

Adam (Kingma & Ba, 2015) with a batch-size of 64, initial learning rate of 3×10^{-4} and weight decay of 10^{-4} are used in training. We use a staircase learning rate schedule with decay milestones at 50% and 75% of the training duration. All instances of both models are trained for 500 epochs using NVIDIA RTX A5000 gpu.

Figure 5 depicts how observed distributions of credit amounts and repayment duration would have changed to the corresponding counterfactual distributions if we hypothetically set the gender of the loanees different from what is reported. While we present the result of counterfactual estimation via 'affine' flow combinations of linear order in Figure 5, the results of other flow combinations are in Appendix C. We also quantitatively compare the associative capabilities of all instances of both models by log-likelihoods (validation) as given in the in the appendix C.

7 Discussion

This paper tackles problem of identifying exogenous noises that must be abducted for counterfactual inference. We demonstrate that identifying noises explicitly is an important task for counterfactual inference as we empirically show that identifying noise variables can reduce the computational load of counterfactual inference without compromising in performance. Identifying exogenous noise variables for answering a counterfactual query also reduce the burden of modelling too many normalizing flows. Our work makes Pawlowski et al. (2020)'s framework applicable to partially specified causal graphs in the setting where we observe all variables that lie in a directed path from X_A to $X_{\mathcal{C}}$ along with their parents. The causal relations among these variables are needed to be fully specified. For example, consider the causal graph in figure 2b. If we are interested in $Y_{X_5 \leftarrow x'_5}(\epsilon)$, it doesn't matter whether X_4 is observed or not. Sub-graph inside the pink region will suffice. Note that we haven't really used X_4 in the partial model of synthetic data experiment as we conditioned on X_3 for answering $Y_{X_5 \leftarrow x'_5}(\epsilon)$.

Though our work is heavily inspired by Pawlowski et al. (2020)'s framework, it is very general to apply to other frameworks for generating counterfactuals. Our work does come with limitations to be investigated further. For example, we don't study the scenario when a hidden (unobserved) variable lies in a path from the intervened variable to the variable we are interested in. We fundamentally don't restrict ourselves from intervening on the variables. In scenarios, where we can't intervene on a variable fundamentally, i.e., when we try to answer the counterfactual queries from observed or a combination of observed and experimental data only, identification of counterfactual questions itself is important. It would be interesting to investigate the roles of the noises in such settings. Another limitation is that reducing the noise abduction set might restrict the generative power of the model[4].

A very noted limitation in counterfactual inference is that for real datasets, counterfactuals are usually unverifiable. Evaluation isn't possible except in a few constrained settings as true counterfactuals are never noticed usually. Counterfactual speculation is what some variable would be in a parallel universe where all but the intervened variables and their descendants were the same. However the machinery of counterfactual inference provides scientists with better schemes for controlling the known confounders. As a result, the SCM framework is widely applicable to enhance trust and the performance ML\AI systems.

References

Andreas Geiger Axel Sauer. Counterfactual generative networks. In *International Conference on Learning Representations (ICLR)*, 2021.

Eli Bingham, Jonathan P. Chen, Martin Jankowiak, Fritz Obermeyer, Neeraj Pradhan, Theofanis Karaletsos, Rohit Singh, Paul Szerlip, Paul Horsfall, and Noah D. Goodman. Pyro: Deep universal probabilistic programming. *J. Mach. Learn. Res.*, 20(1):973–978, jan 2019. ISSN 1532-4435.

Riccardo Crupi, Alessandro Castelnovo, Daniele Regoli, and Beatriz San Miguel Gonzalez. Counterfactual explanations as interventions in latent space. *arXiv preprint arXiv:2106.07754*, 2021.

Saloni Dash, Vineeth N. Balasubramanian, and Amit Sharma. Evaluating and mitigating bias in image classifiers: A causal perspective using counterfactuals. In *IEEE/CVF Winter Conference on Applications of Computer Vision, WACV 2022, Waikoloa, HI, USA, January 3-8, 2022*, pp. 3879–3888. IEEE, 2022. doi: 10.1109/WACV51458.2022.00393. URL https://doi.org/10.1109/WACV51458.2022.00393.

Laurent Dinh, Jascha Sohl-Dickstein, and Samy Bengio. Density estimation using real NVP. In *5th International Conference on Learning Representations, ICLR 2017, Toulon, France, April 24-26, 2017, Conference Track Proceedings*. OpenReview.net, 2017. URL https://openreview.net/forum?id=HkpbnH9lx.

Hadi Mohaghegh Dolatabadi, Sarah Erfani, and Christopher Leckie. Invertible generative modeling using linear rational splines. In *The 23rd International Conference on Artificial Intelligence and Statistics (AISTATS)*, pp. 4236–4246, 2020.

[4]Discussed in appendix B

Dheeru Dua and Casey Graff. UCI machine learning repository, 2017. URL http://archive.ics.uci.edu/ml.

Conor Durkan, Artur Bekasov, Iain Murray, and George Papamakarios. Neural spline flows. In H. Wallach, H. Larochelle, A. Beygelzimer, F. d'Alché-Buc, E. Fox, and R. Garnett (eds.), *Advances in Neural Information Processing Systems*, volume 32. Curran Associates, Inc., 2019. URL https://proceedings.neurips.cc/paper/2019/file/7ac71d433f282034e088473244df8c02-Paper.pdf.

Amir-Hossein Karimi, Bernhard Schölkopf, and Isabel Valera. Algorithmic recourse: from counterfactual explanations to interventions. *Proceedings of the 2021 ACM Conference on Fairness, Accountability, and Transparency*, 2021.

Diederik P. Kingma and Jimmy Ba. Adam: A method for stochastic optimization. In Yoshua Bengio and Yann LeCun (eds.), *3rd International Conference on Learning Representations, ICLR 2015, San Diego, CA, USA, May 7-9, 2015, Conference Track Proceedings*, 2015. URL http://arxiv.org/abs/1412.6980.

Matt J Kusner, Joshua Loftus, Chris Russell, and Ricardo Silva. Counterfactual fairness. In I. Guyon, U. Von Luxburg, S. Bengio, H. Wallach, R. Fergus, S. Vishwanathan, and R. Garnett (eds.), *Advances in Neural Information Processing Systems*, volume 30. Curran Associates, Inc., 2017. URL https://proceedings.neurips.cc/paper/2017/file/a486cd07e4ac3d270571622f4f316ec5-Paper.pdf.

Daniel Malinsky, Ilya Shpitser, and Thomas Richardson. A potential outcomes calculus for identifying conditional path-specific effects, 2019. URL https://arxiv.org/abs/1903.03662.

Guilherme F. Marchezini, Anisio M. Lacerda, Gisele L. Pappa, Wagner Meira, Debora Miranda, Marco A. Romano-Silva, Danielle S. Costa, and Leandro Malloy Diniz. Counterfactual inference with latent variable and its application in mental health care. *Data Min. Knowl. Discov.*, 36(2):811–840, mar 2022. ISSN 1384-5810. doi: 10.1007/s10618-021-00818-9. URL https://doi.org/10.1007/s10618-021-00818-9.

Yulei Niu, Kaihua Tang, Hanwang Zhang, Zhiwu Lu, Xiansheng Hua, and Ji rong Wen. Counterfactual vqa: A cause-effect look at language bias. *2021 IEEE/CVF Conference on Computer Vision and Pattern Recognition (CVPR)*, pp. 12695–12705, 2021.

George Papamakarios, Eric Nalisnick, Danilo Jimenez Rezende, Shakir Mohamed, and Balaji Lakshminarayanan. Normalizing flows for probabilistic modeling and inference. 2019. doi: 10.48550/ARXIV.1912.02762. URL https://arxiv.org/abs/1912.02762.

Adam Paszke, Sam Gross, Francisco Massa, Adam Lerer, James Bradbury, Gregory Chanan, Trevor Killeen, Zeming Lin, Natalia Gimelshein, Luca Antiga, Alban Desmaison, Andreas Köpf, Edward Yang, Zach DeVito, Martin Raison, Alykhan Tejani, Sasank Chilamkurthy, Benoit Steiner, Lu Fang, Junjie Bai, and Soumith Chintala. *PyTorch: An Imperative Style, High-Performance Deep Learning Library*. Curran Associates Inc., Red Hook, NY, USA, 2019.

Nick Pawlowski, Daniel Coelho de Castro, and Ben Glocker. Deep structural causal models for tractable counterfactual inference. In H. Larochelle, M. Ranzato, R. Hadsell, M.F. Balcan, and H. Lin (eds.), *Advances in Neural Information Processing Systems*, volume 33, pp. 857–869. Curran Associates, Inc., 2020. URL https://proceedings.neurips.cc/paper/2020/file/0987b8b338d6c90bbedd8631bc499221-Paper.pdf.

Judea Pearl. *Causality*. Cambridge University Press, 2 edition, 2009. doi: 10.1017/CBO9780511803161.

Judea Pearl. *Causal inference in statistics : a primer*. John Wiley & Sons Ltd, Chichester, West Sussex, UK, 2016. ISBN 1119186854.

J. Peters, D. Janzing, and B. Schölkopf. *Elements of Causal Inference - Foundations and Learning Algorithms*. Adaptive Computation and Machine Learning Series. The MIT Press, Cambridge, MA, USA, 2017.

Jacob C. Reinhold, Aaron Carass, and Jerry L. Prince. A structural causal model for mr images of multiple sclerosis. In *Medical Image Computing and Computer Assisted Intervention – MICCAI 2021*, pp. 782–792, Cham, 2021. Springer International Publishing.

Jonathan G. Richens, Rory Beard, and Daniel H. Thompson. Counterfactual harm, 2022. URL https://arxiv.org/abs/2204.12993.

Pedro Sanchez and Sotirios A. Tsaftaris. Diffusion causal models for counterfactual estimation. *CoRR*, abs/2202.10166, 2022. URL https://arxiv.org/abs/2202.10166.

Bernhard Schölkopf. Causality for machine learning, 2019. URL https://arxiv.org/abs/1911.10500.

Jin Tian and Judea Pearl. Causal discovery from changes, 2013. URL https://arxiv.org/abs/1301.2312.

Jan-Willem van de Meent, Brooks Paige, Hongseok Yang, and Frank Wood. An introduction to probabilistic programming, 2018. URL https://arxiv.org/abs/1809.10756.

Rongguang Wang, Pratik Chaudhari, and Christos Davatzikos. Harmonization with flow-based causal inference. In *Medical Image Computing and Computer Assisted Intervention – MICCAI 2021*, pp. 181–190, Cham, 2021. Springer International Publishing. ISBN 978-3-030-87199-4.

Zhongqi Yue, Tan Wang, Hanwang Zhang, Qianru Sun, and Xiansheng Hua. Counterfactual zero-shot and open-set visual recognition. *2021 IEEE/CVF Conference on Computer Vision and Pattern Recognition (CVPR)*, pp. 15399–15409, 2021.

Cheng Zhang, Kun Zhang, and Yingzhen Li. A causal view on robustness of neural networks. In H. Larochelle, M. Ranzato, R. Hadsell, M.F. Balcan, and H. Lin (eds.), *Advances in Neural Information Processing Systems*, volume 33, pp. 289–301. Curran Associates, Inc., 2020. URL https://proceedings.neurips.cc/paper/2020/file/02ed812220b0705fabb868ddbf17ea20-Paper.pdf.